



**Providing Choice & Value**  
Generic CT and MRI Contrast Agents



CONTACT REP

# AJNR

## **MELAS: Phenotype Classification into Classic-versus-Atypical Presentations**

C.A.P.F. Alves, A. Zandifar, J.T. Peterson, S.Z. Tara, R. Ganetzky, A.N. Viaene, S. Andronikou, M.J. Falk, A. Vossough and A.C. Goldstein

This information is current as of July 31, 2025.

*AJNR Am J Neuroradiol* published online 6 April 2023  
<http://www.ajnr.org/content/early/2023/04/06/ajnr.A7837>

# MELAS: Phenotype Classification into Classic-versus-Atypical Presentations

 C.A.P.F. Alves,  A. Zandifar,  J.T. Peterson,  S.Z. Tara,  R. Ganetzky,  A.N. Viaene,  S. Andronikou,  M.J. Falk,  A. Vossough, and  A.C. Goldstein



## ABSTRACT

**BACKGROUND AND PURPOSE:** An increased number of pathogenic variants have been described in mitochondrial encephalomyopathy lactic acidosis and strokelike episodes (MELAS). Different imaging presentations have emerged in parallel with a growing recognition of clinical and outcome variability, which pose a diagnostic challenge to neurologists and radiologists and may impact an individual patient's response to therapeutic interventions. By evaluating clinical, neuroimaging, laboratory, and genetic findings, we sought to improve our understanding of the sources of potential phenotype variability in patients with MELAS.

**MATERIALS AND METHODS:** This retrospective single-center study included individuals who had confirmed mitochondrial DNA pathogenic variants and a diagnosis of MELAS and whose data were reviewed from January 2000 through November 2021. The approach included a review of clinical, neuroimaging, laboratory, and genetic data, followed by an unsupervised hierarchical cluster analysis looking for sources of phenotype variability in MELAS. Subsequently, experts identified "victory-variables" that best differentiated MELAS cohort clusters.

**RESULTS:** Thirty-five patients with a diagnosis of mitochondrial DNA–based MELAS (median age, 12 years; interquartile range, 7–24 years; 24 female) were eligible for this study. Fifty-three discrete variables were evaluated by an unsupervised cluster analysis, which revealed that two distinct phenotypes exist among patients with MELAS. After experts reviewed the variables, they selected 8 victory-variables with the greatest impact in determining the MELAS subgroups: developmental delay, sensorineural hearing loss, vision loss in the first strokelike episode, Leigh syndrome overlap, age at the first strokelike episode, cortical lesion size, regional brain distribution of lesions, and genetic groups. Ultimately, 2-step differentiating criteria were defined to classify atypical MELAS.

**CONCLUSIONS:** We identified 2 distinct patterns of MELAS: classic MELAS and atypical MELAS. Recognizing different patterns in MELAS presentations will enable clinical and research care teams to better understand the natural history and prognosis of MELAS and identify the best candidates for specific therapeutic interventions.

**ABBREVIATIONS:** CSLL = cortical strokelike lesion; LS = Leigh syndrome; MELAS = mitochondrial encephalomyopathy lactic acidosis and strokelike episodes; mtDNA = mitochondrial DNA; mt-tRNA = mitochondrial tRNA; SLE = strokelike episode; SNHL = sensorineural hearing loss

Mitochondrial encephalomyopathy lactic acidosis and strokelike episodes (MELAS) is considered a canonical mitochondrial disorder,<sup>1,2</sup> primarily caused by pathogenic variants

in mitochondrial DNA (mtDNA), though few nuclear genes have been considered.<sup>3–5</sup>

A 2012 study updated the clinical criteria for MELAS diagnosis from the previous ones, described in 1992.<sup>6,7</sup> The current criteria include at least 2 category A and at least two category B criteria. Category A is based on clinical symptoms and neuroimaging findings, including headaches with vomiting, seizures, hemiplegia, cortical blindness, and acute focal lesions involving the brain cortex.<sup>7,8</sup> Category B is based on laboratory results showing increased plasma or CSF lactate, mitochondrial abnormalities on muscle biopsy, and a MELAS-related pathogenic variant on genetic testing. Although these well-defined MELAS diagnostic criteria have been established, there is still large clinical, imaging, and outcome variability among patients with a diagnosis of MELAS.<sup>9</sup>

The *MT-TL1* m.3243A>G is considered the most common pathogenic variant identified with MELAS.<sup>10,11</sup> However, reports

Received December 22, 2022; accepted after revision February 24, 2023.

From the Division of Neuroradiology (C.A.P.F.A., A.Z., S.A., A.V.), Department of Radiology; Mitochondrial Medicine Frontier Program (J.T.P., S.Z.T., R.G., M.J.F., A.C.G.), Division of Human Genetics, Department of Pediatrics; and Department of Pathology and Laboratory Medicine (A.N.V.), The Children's Hospital of Philadelphia, Philadelphia, Pennsylvania; and Departments of Pediatrics (R.G., M.J.F., A.C.G.), Pathology and Laboratory Medicine (A.N.V.), and Radiology (S.A., A.V.), Perelman School of Medicine, University of Pennsylvania Perelman School of Medicine, Philadelphia, Pennsylvania.

C.A.P.F. Alves and A. Zandifar contributed equally to this work.

A. Vossough and A.C. Goldstein shared the last authorship.

Please address correspondence to Cesar Augusto Alves, MD, PhD, Division of Neuroradiology, Department of Radiology, Children's Hospital of Philadelphia, 324 South 34th St, Philadelphia, PA 19104; e-mail: alvesc@chop.edu; @cesaralvesneuro

 Indicates article with online supplemental data.

<http://dx.doi.org/10.3174/ajnr.A7837>

show that the phenotype has a more diverse and heterogeneous clinical spectrum, even within families.<sup>12-15</sup> Moreover, other mtDNA causes of MELAS include but are not limited to variants such as m.3271T>C and m.3252A>G in *MT-TL1*. Recently, MELAS has been described with other mtDNA genes, particularly those linked to the mitochondrial respiratory chain complex subunits involved with oxidative phosphorylation.<sup>9,16,17</sup> In parallel with the clinical and genetic variability, new imaging manifestations are being recognized. Mitochondrial experts believe these advances warrant a better, more granular delineation of this disorder and a revision of the current diagnostic criteria, which may have direct implications for appropriate management and formulation of clinical trials. Therefore, we sought to investigate the variations in clinical features, brain MR imaging, laboratory and genetic findings, and outcome differences in a mtDNA-based MELAS cohort to provide an updated and comprehensive classification of this disorder.

## MATERIALS AND METHODS

### Setting and Participants

We designed this retrospective study according to the Strengthening the Reporting of Observational Studies in Epidemiology statement.<sup>18</sup> The institutional review board (The Children's Hospital of Philadelphia) approved this study, and informed consent was obtained. Brain MRIs were retrieved from January 2000 to November 2021. We identified clinical cases from the Mitochondrial Medicine Frontier Program. All individuals with a diagnosis followed and treated as MELAS at our institution who had an available MR imaging were included. All included individuals had a genetically confirmed primary mitochondrial disorder due to any pathogenic mtDNA variant with a heteroplasmy level of >30% in at least 1 tested tissue.<sup>19</sup> Individuals with nuclear DNA etiologies were excluded.

### Clinical and Outcome Data

Symptoms presenting from the onset of the disorder until the last visit were recorded. One pediatric neurologist (A.C.G.) specializing in mitochondrial disorders with 20 years of experience reviewed the medical records to confirm the diagnosis and the accuracy of the collected clinical data.

### Genetic, Laboratory, and Histopathology Data

A genetic counselor (J.T.P.) reviewed genetic analyses performed to confirm the pathogenic variants. Patients with nuclear DNA etiologies causing stroke-like episodes were not included in this MELAS cohort because they likely have distinct pathogenesis and may represent a better clinically-defined entity such as *POLG*-related disorders.<sup>20,21</sup> Comprehensive mtDNA genome sequencing was completed via next-generation sequencing for most of the cohort (31/35). Four of 35 individuals had only historical results available and had either Sanger sequencing, real-time amplification refractory mutation system polymerase chain reaction, or HaeIII restriction digest testing for m.3243A>G. The maternal inheritance pattern was confirmed when parental samples were available and the proband had clinical and MR imaging findings supporting a diagnosis of MELAS. Laboratory data (highest lifetime plasma, CSF lactate, and plasma alanine) were noted when available. A

pediatric neuropathologist (A.N.V.) reviewed any available pathology specimen results.

### MR Imaging

MR imaging was performed on a variety of 1.5T and 3T scanners (Siemens, GE Healthcare, Philips Healthcare). Detailed imaging protocol and parameters can be found in a previous article published by our group.<sup>9</sup> Additional sequences including single-voxel <sup>1</sup>H-MR spectroscopy, postcontrast axial T1-weighted imaging, arterial spin-labeling, SWI, and DTI were assessed when available.

Brain MR imaging, previously performed for clinical purposes, was independently reviewed by 2 neuroradiologists (C.A.P.F.A. and A.V.). MR imaging examinations were reviewed on clinical-grade viewing software, and data were collected using a standardized form. Reviewers were blinded to patients' genetic and clinical features, but not to the primary diagnosis. MR imaging findings were described according to their signal-intensity characteristics and location in the brain. For cortical lesions, in addition to the overall description, further classification was based on the presence of small (<30 mm) and/or large (≥30 mm) cortical stroke-like lesions (CSLLs) and number, symmetry, anatomic and regional distribution of the lesions (frontal and anterior parietal lobes were considered the anterior region, and posterior parietal, insula, occipital, and temporal lobes, were considered posterolateral regions), and the presence of subcortical white matter extension. CSLLs were measured in their largest anterior-posterior extension in the axial plane using FLAIR and/or DWI sequences.

### Unsupervised Clustering Analysis

All potential variables, including clinical, laboratory, and imaging data, were pooled. We performed an unsupervised hierarchical cluster analysis to expose any potential phenotype patterns across cases of MELAS. To evaluate differences in variable frequencies among the clusters, we compared all included variables using appropriate statistical tests. In the second step, we calculated the agglomerative coefficient of our clustering before and after removing each variable to find its contribution size. According to agglomerative coefficient changes, we selected the strongest variables to differentiate the subgroups. On the basis of the modified variable list, the final agglomerative coefficient was calculated to confirm the optimization of our cluster analysis. The association between the assigned clusters and the genetic data was assessed at this step. To ensure the quality of clustering, we used the average silhouette method to confirm the optimal number of clusters.

### Expert Panel

A team of mitochondrial medicine specialists was invited to the expert panel. They were provided with a summary of unidentified patient data and were asked to categorize patients into classic MELAS or an atypical phenotype based on the modified variable list. The experts were blinded to the results of unsupervised clustering during categorization. Furthermore, they indicated which modified variables played an important role in categorization and could be considered "victory-variables" to differentiate the clusters. Finally, the expert clustering was compared with the results of the unsupervised cluster analysis. To define the differentiating

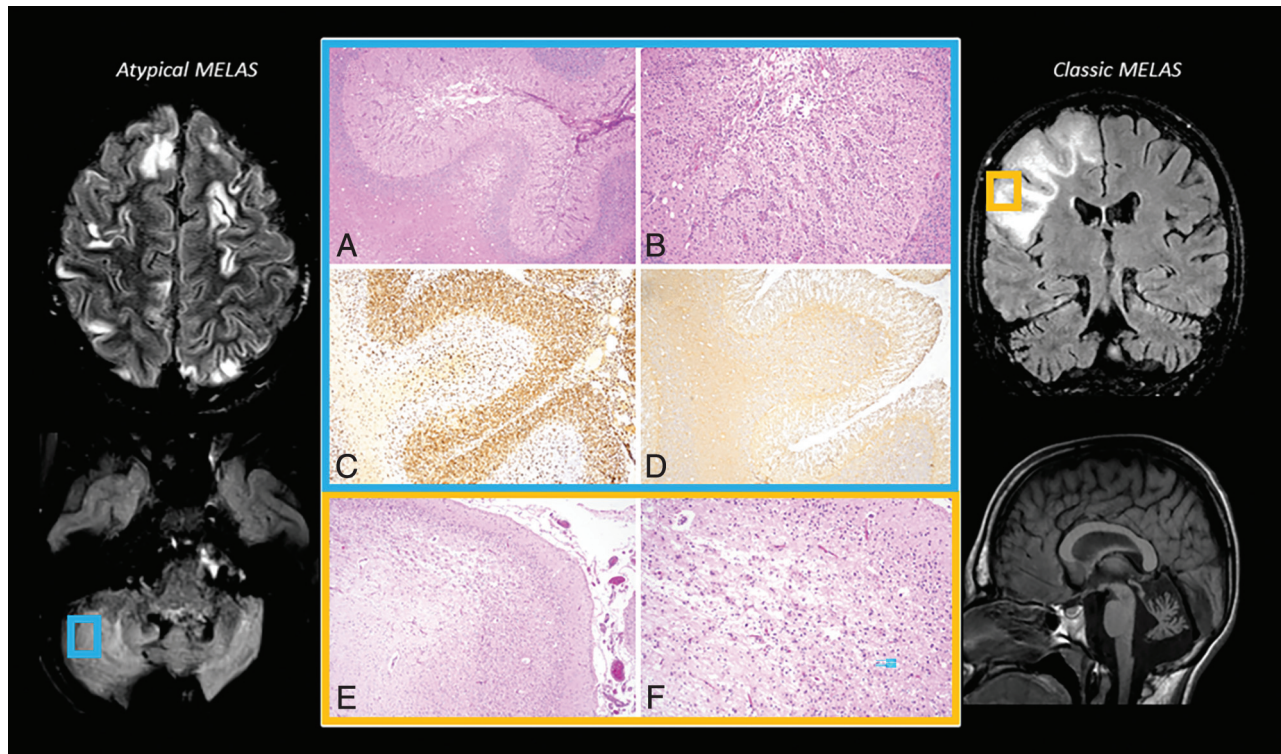


**FIG 1.** A, Biopsy of the cerebellum showing a subacute infarct involving the folia (H&E stain, original magnification  $\times 40$ ). B, Higher magnification of the subacute infarct. There is rarefaction, marked vascular proliferation, and macrophage collections within the molecular layer as well as loss of Purkinje neurons (H&E stain, original magnification  $\times 100$ ). C, CD68 immunostain demonstrates numerous macrophages within the molecular layer (CD68 immunostain, original magnification  $\times 40$ ). D, Glial fibrillary acidic protein (GFAP) highlights reactive gliosis (GFAP immunostain, original magnification  $\times 40$ ). E, Postmortem tissue from a second, classic MELAS patient demonstrates the cortex with an infarct involving the gyral crest (H&E stain, original magnification  $\times 40$ ). F, Higher magnification image of the infarct shows neuronal loss, tissue rarefaction, and gliosis (H&E stain, original magnification  $\times 200$ ).

criteria, we weighted victory-variables according to their specificity, and score cutoffs were determined to differentiate classic MELAS from atypical MELAS.

### Longitudinal Evaluation

Individuals were evaluated longitudinally to determine their clinical course and prognosis based on medical complications and the pattern of progression of the neuroimaging findings. Poor clinical prognosis was defined as respiratory failure and bulbar dysfunction. Survival at last evaluation or age at death or both were determined. For the neuroimaging pattern of progression, the interval appearance of new lesions, increased size of previously detected lesions, and extensive volume loss from baseline MR imaging to the last MR imaging study were defined as poor outcomes.

### Statistical Data

Data were analyzed using R statistical and computing software (Version 3.5.1; <http://www.r-project.org/>), SPSS Statistics for Windows (Version 26.0; IBM), and MedCalc Software odds ratio calculator (Version 20.106; [https://www.medcalc.org/calc/odds\\_ratio.php](https://www.medcalc.org/calc/odds_ratio.php)). Numeric variables were described according to their distribution with median and interquartile range and were compared using the Mann-Whitney  $U$  test. Categorical variables were expressed as percentages and frequency and were compared using the Fisher exact test and an OR with a 95% CI. Two-sided

$P$  values  $< .01$  were considered statistically significant. Kaplan-Meier curves and log-rank tests were used to determine the differences in the occurrence of respiratory failure and bulbar dysfunction between different types of MELAS.

### RESULTS

One hundred twenty-one of 237 patients with a confirmed mitochondrial disorder had brain MRIs available for review. Thirty-five of these 121 individuals had a diagnosis of MELAS and pathogenic mtDNA variants.<sup>6</sup> Our cohort had a median age at symptom onset of 10 years (interquartile range = 4–19 years) and a male/female ratio of 2.2:1. A total of 79 brain MRIs (baseline and follow-up studies) were available. Follow-up MRIs were accessed for 26 of 35 (74%) individuals. Longitudinal clinical data were available for all patients. At the time of this analysis, 3 of 35 patients were deceased with the ages of death at 0.1, 1.8, and 7 years. Two had brain pathology specimens (1 surgical biopsy and 1 postmortem) available that showed indistinguishable infarctions consistent with vasculonecrotic lesions and vascular mitochondrial dysfunction (Fig 1). Demographic, clinical, laboratory, and genetic data are summarized in the Online Supplemental Data.

The schematic workflow of the successive steps is shown in Fig 2. Fifty-three variables were evaluated by unsupervised cluster analysis and visualized through a heatmap, which revealed 2

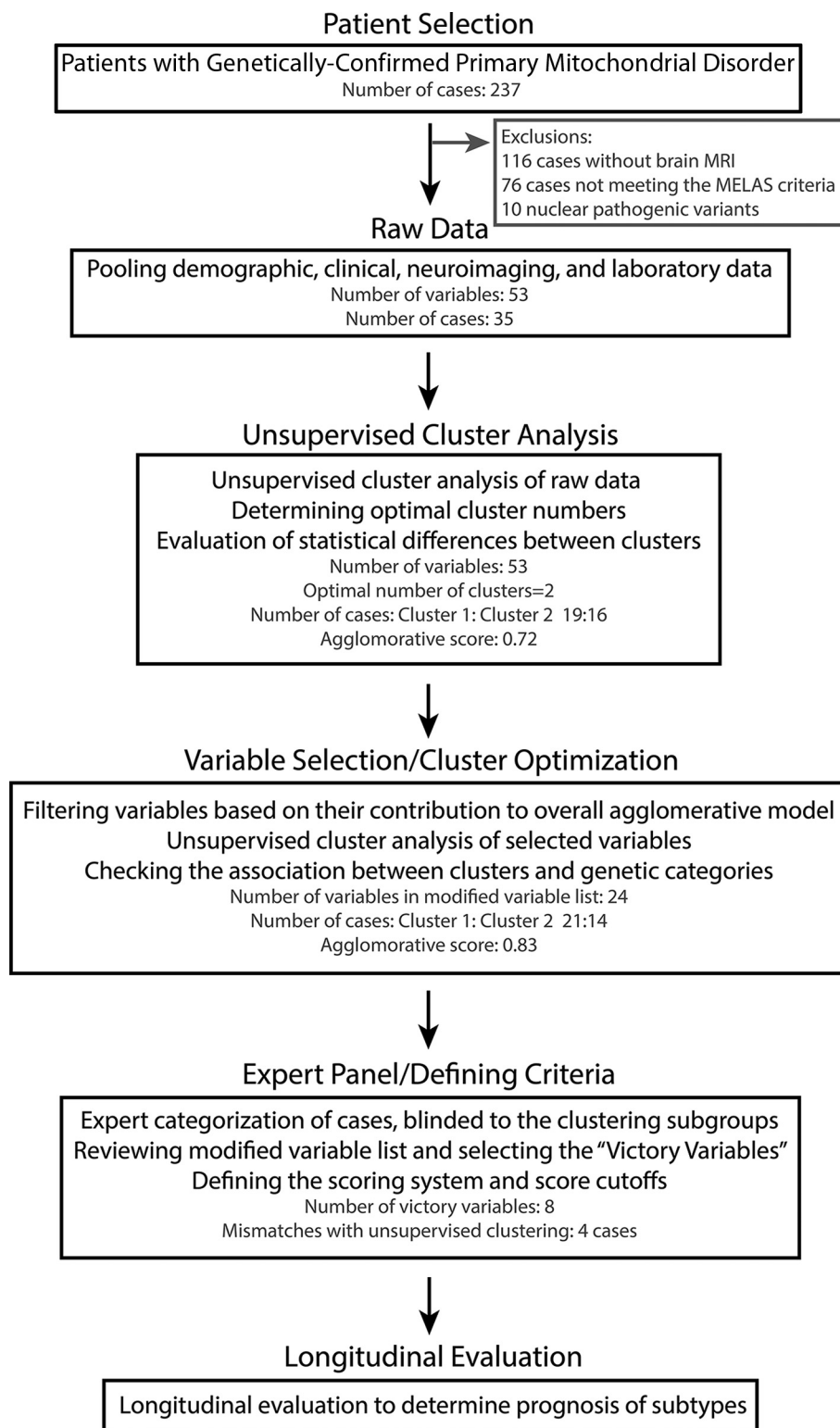


**FIG 2.** Work flow diagram. yo indicates years of age.

phenotype patterns among the mtDNA-based MELAS cohort (Online Supplemental Data). The average silhouette confirmed 2 to be the optimal number of cohort subgroups (Online Supplemental Data). When comparing the frequency of included variables between the 2 clusters, we found differences in 18 of 53 variables (all with  $P$  value  $< .01$ ) (Online Supplemental Data). In the

second step, agglomerative scores of the clusters were calculated before and after removing each variable, and 24 variables with a positive contribution were selected to optimize the clusters. The overall agglomerative score of the clustering changed from 0.72 to 0.83, with more distinct patterns of the variables evident in the visual heatmap (Fig 3). Comparing the results of unsupervised

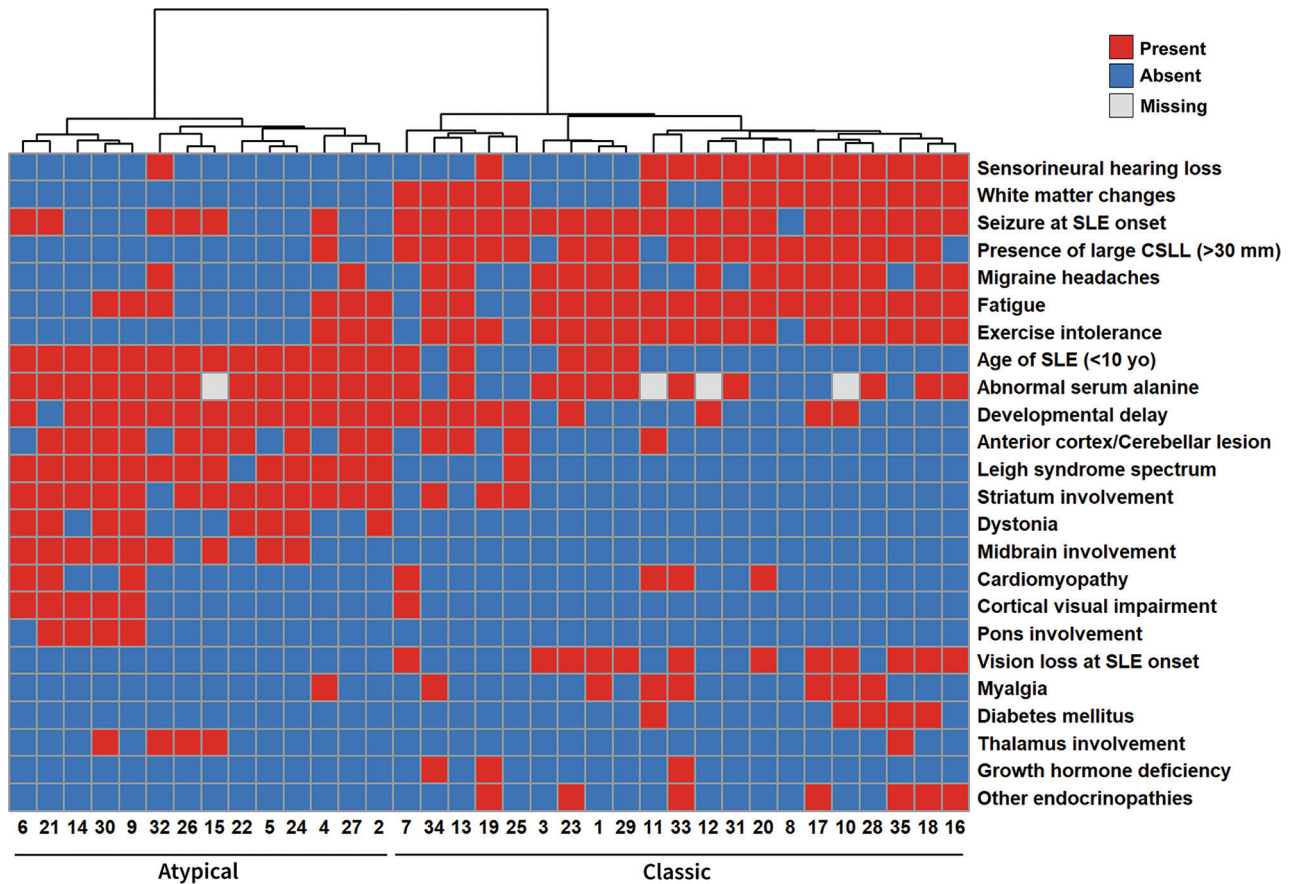


**FIG 3.** Unsupervised cluster analysis of the binary data based on the modified variable list (y-axis) using the Ward hierarchic clustering method. Each column represents 1 patient (x-axis). Red and blue squares show the presence and absence of the findings in each patient, respectively. At the top of the heatmap, the height of the dendrogram for main clusters demonstrates the high distance between clusters, which confirms the 2 distinct patterns of disease.

cluster analysis with the genetic data demonstrated that the mitochondrial tRNA (mt-tRNA) variants were more associated with one of the clusters while respiratory chain subunit genes were associated with the other cluster (OR = 26; 95% CI, 2.8–241;  $P$  value = .001).

Subsequently, the experts, blinded to the distribution of cases, were asked to categorize the patients into 2 subtypes using the 24 variables and the genetic data. The expert categorization results were then compared with the cluster subgroups, which showed 31 agreements and 4 discrepancies in assigning the individuals into 2 categories.

To enrich the clustering with clinical judgment, the experts reviewed the 24 variables and selected the most discriminating to differentiate MELAS subgroups from clinical, neuroimaging, and genetic perspectives, noteworthy all with  $P$  value < .01. Eight variables were selected as victory-variables. These victory-variables included the following: A) 5 clinical and demographic findings: 1) developmental delay, 2) sensorineural hearing loss (SNHL), 3) vision loss at stroke-like episode (SLE) onset, 4) overlap with Leigh syndrome (LS) as defined by additional symptoms of dystonia and brain lesions in the basal ganglia and/or brainstem, and 5) age at first SLE (10 years or younger versus older than 10 years of age); B) 2 neuroimaging variables: 1) the presence of large CSLLs ( $\geq 30$  mm), and 2) regional lesion distribution (anterior

and/or cerebellar versus posterolateral involvement, as previously defined); and C) 1 pathogenic variant category: gene categories involving the mt-tRNA variants or respiratory chain subunit genes. According to these variables, 2 subgroups of MELAS were defined.

Classic MELAS was associated with SNHL, vision loss at the onset of SLE, the first SLE occurring at older than 10 years of age, the presence of large CSLLs ( $\geq 30$  mm), and the mt-tRNA variant gene group. Atypical MELAS was associated with developmental delay, LS overlap, the first SLE at 10 years of age or younger, small CSLLs, cortical lesions predominantly located in anterior regions of the brain (frontal and anterior parietal lobes) and cerebellar cortex (the latter particularly in the context of *MT-ATP6* variants), and belonging to the respiratory chain subunit gene group (Fig 4). There were no differences among the subgroups based on other imaging features, including other cortical changes,<sup>22</sup> number of areas with hyper- or hypoperfusion on arterial spin-labeling, MR spectroscopy, iron deposition, or cerebellar atrophy.

Ultimately, using the victory-variables, we defined a 2-step criterion to differentiate the subtypes generated by the cluster analysis. The first step was to calculate a score on the basis of 5 clinical and 2 neuroimaging findings. The second step involved using genetic data for equivocal cases. On the basis of the specificity of victory-variables, LS overlap and SNHL were weighted

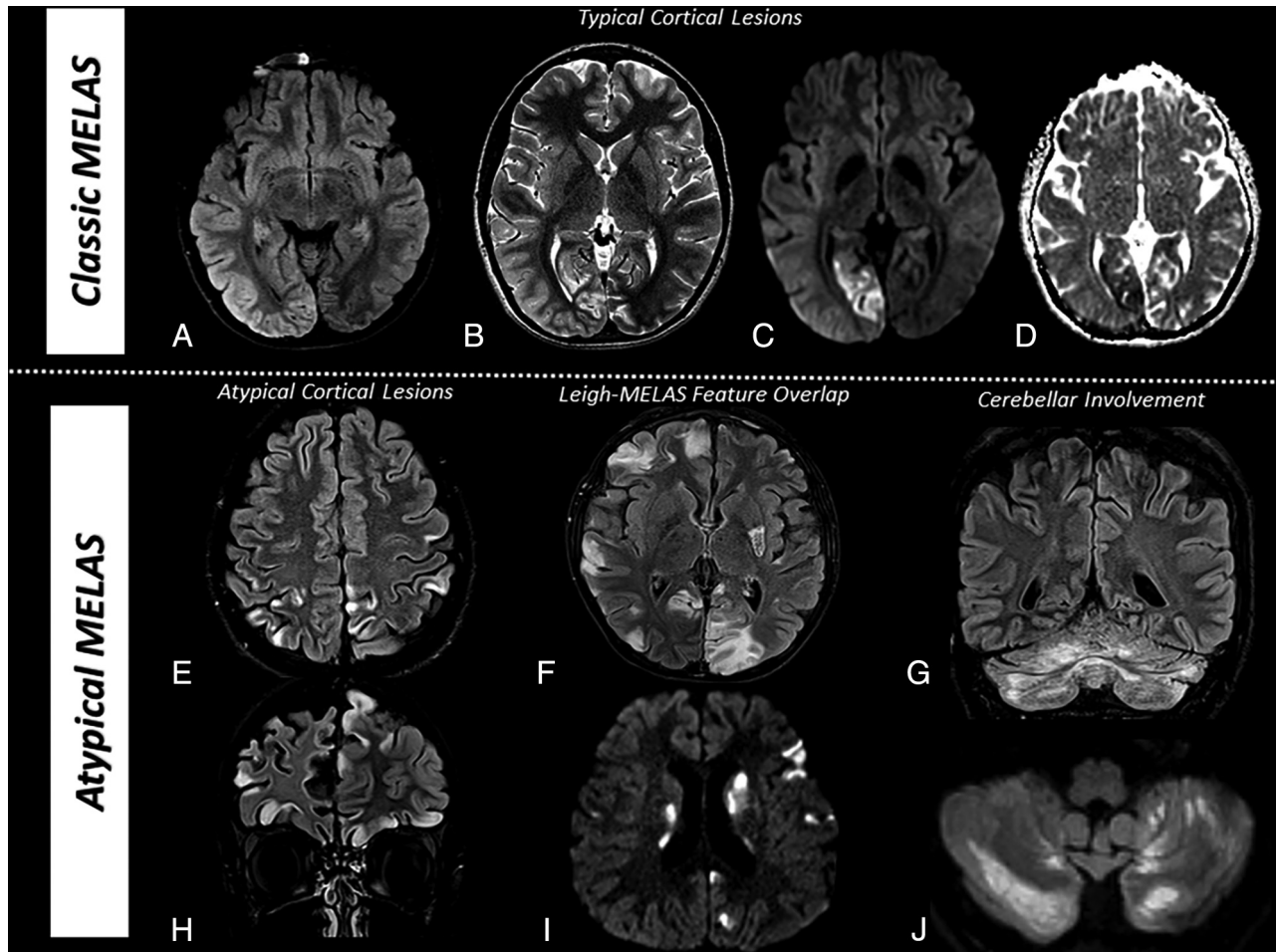


**FIG 4.** Classic MELAS. A large unique cortical lesion involves the right occipital and temporal lobes (posterolateral region of the brain) with FLAIR and T2 hyperintensity (A and B) and components of restricted diffusion in the medial occipital lobe confirmed in the ADC MAP (C and D). Atypical MELAS. Scattered, multiple, small cortical lesions involving both frontal and parietal lobes with FLAIR hyperintensity (E–H). Atypical MELAS with LS overlap. Multiple scattered cortical lesions with subcortical extension in association with basal ganglia involvement, configuring LS overlap, with FLAIR hyperintensity (F) and some areas of restricted diffusion (I) confirmed in the ADC MAP, not shown. Atypical MELAS with predominant cerebellar involvement. Cerebellar FLAIR hyperintensity (G) and components of restricted diffusion (J) were confirmed in the ADC MAP, not shown.

twice (high accuracy variables for cluster differentiation) relative to the other variables. The overall score (range from  $-4$  to  $+5$ ) was calculated for each case, and score cutoffs were defined to differentiate classic MELAS from atypical MELAS. The calculated score of  $\leq -2$  was defined as classic MELAS and  $\geq +2$  was defined as atypical MELAS. Scores between  $-1$  and  $+1$  were considered equivocal, which included cases in which the expert opinion and the cluster data were incompatible. In these cases, the genetic data were used as a confirmatory method to define the final subtype of mtDNA-based MELAS (Table 1).

Longitudinal evaluation showed that patients diagnosed with atypical MELAS based on the defined criteria had a higher chance of experiencing respiratory failure [ $\chi^2(1) = 4.686, P = .03$ ] and bulbar dysfunction [ $\chi^2(1) = 10.885, P = .001$ ] during the course of their disease (Fig 5). Among 3 deceased individuals, 2 had atypical and 1 had classic MELAS. Neuroimaging follow-up studies showed that atypical MELAS was more often associated with an increasing number of CSLs during the disease course (OR = 24; 95% CI, 1.04–559;  $P = .006$ ).

## DISCUSSION

While MELAS is a well-established mitochondrial disorder with a generally recognizable clinical phenotype, the clinical, imaging, genetic, and outcome variability of this complex syndrome remains underrecognized. In this study, 2 subgroups of MELAS were defined in a cohort of patients with MELAS on the basis of key clinical, neuroimaging, and genetic categories. The constellation of multiple variables from these 3 categories was evaluated, and 8 victory-variables were selected. The 8 victory-variables encompassed the following: A) 5 clinical/demographic variables: age of the first SLE, SNHL, developmental delay, vision loss occurring at onset of SLE, and overlap with LS; B) 2 neuroimaging variables: an anterior scattered region (frontal and anterior parietal lobes) and/or cerebellar-versus-posterolateral (temporo-occipital lobes) involvement, and cortical lesion size on the baseline MR imaging; and C) 1 genetic variable: gene categories involving the mt-tRNA variants or respiratory chain subunit genes.

Atypical MELAS was associated with symptoms occurring at a younger age (SLE at younger than 10 years of age) and

### Two-step differentiating criteria for distinguishing atypical MELAS from classic MELAS<sup>a</sup>

Finding Category	Findings	Score
Step 1		
Demographic	First strokelike episode at younger than 10 years of age	+1
Clinical	Vision loss at strokelike episode onset	-1
Clinical	Overlap with LS spectrum	+2
Clinical	SNHL	-2
Clinical	Developmental delay	+1
Neuroimaging	Scattered, anterior/cerebellar lesions	+1
Neuroimaging	Presence of large CSLLs (>30 mm) <sup>b</sup>	-1
Step 2 (If -1 ≤ score ≤ 1)		
Genetic	Respiratory chain subunit gene group is most likely associated with atypical MELAS; mt-tRNA genes group is most likely associated with classic MELAS	

<sup>a</sup>Score ≥2: atypical MELAS, score ≤ -2: classic MELAS. If -1 ≤ score ≤ 1: equivocal (genetic study should be considered) → Step 2.

<sup>b</sup>CSLLs measured in their largest anterior-posterior extension in the axial plane using FLAIR and/or DWI sequences.

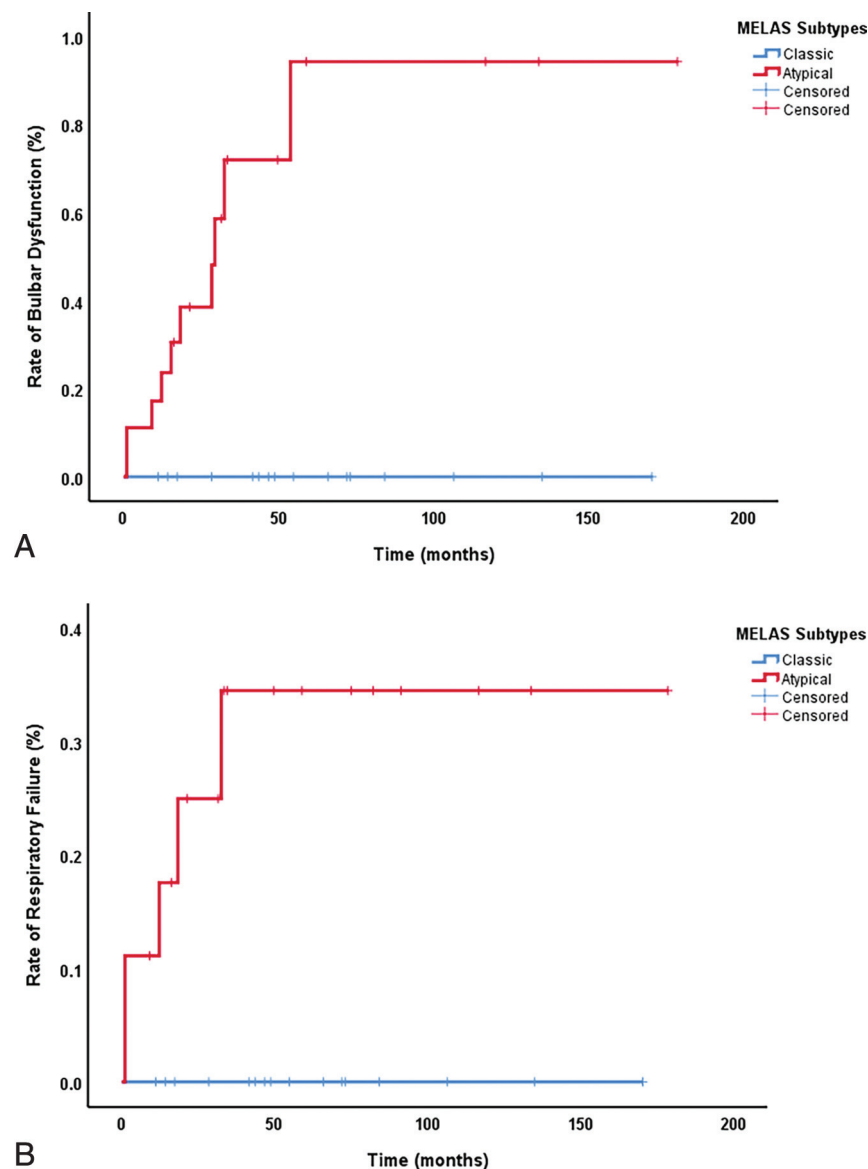


**FIG 5.** A, Clinical outcome (rates of bulbar dysfunction between MELAS subgroups). B, Clinical outcome (rates of respiratory failure between MELAS subgroups).

developmental delay, while classic MELAS was associated with SNHL and vision loss occurring at the first SLE.<sup>6,23</sup> Although not part of the victory-variables, other important clinical differences should be considered to distinguish between subtypes of MELAS, including diabetes mellitus and migraine, which demonstrated significant differences in this study and are associated with classic MELAS.<sup>24-26</sup> Conditions of individuals with the classic form of MELAS were rarely associated with LS (6%), while this overlap was frequent in the atypical MELAS subgroup (80%). Following a complex clinical variability, LS/MELAS overlap included mostly individuals presenting with additional symptoms of dystonia and the neuroimaging criteria for LS, including lesions in the basal ganglia and/or brainstem.<sup>9</sup>

Consistent with reported literature, the genetic category analysis showed that mt-tRNA variants, particularly *MT-TL1* m.3243 A > G, were observed in classic MELAS.<sup>13,14</sup> In contrast, respiratory chain subunit genes were associated with atypical MELAS, specifically variants in complex I (*MT-ND1*, *MT-ND3*, *MT-ND5*) and complex V (*MT-ATP6*, *MT-ATP8*) subunits. Even though genes involving the respiratory chain subunits have been established in association with MELAS,<sup>9</sup> most of these genes are known to be causally related to LS.<sup>27</sup> In our cohort, the genetic results were predictive of clinical and radiologic phenotypes. However, there were exceptions seen, including 1 patient with the *MT-TL1* variant presenting with atypical MELAS and 2 patients with subunit genetic variants (*MT-CYB*, *MT-ND5*) presenting with classic MELAS.

Neuroimaging findings with corresponding imaging symptoms play a critical role in the definition of MELAS, often revealing a characteristic pattern of disappearing and relapsing large CSLLs in the brain.<sup>28</sup> These lesions are characteristically located in the occipital, posterior parietal, or temporal lobes, not respecting vascular territories.<sup>28,29</sup> We observed that large lesions mainly involving the occipital and temporal lobes were associated with classic MELAS, similar to findings in the literature.<sup>28,29</sup> Atypical patterns of CSLL,

including smaller size, lower frequency of posterolateral distribution, and higher frequency of cerebellar involvement were noted in atypical MELAS. Additional association was noted between cerebellar lesions (with or without supratentorial cortical involvement) and *MT-ATP6* variants in the context of atypical MELAS. Surveillance MR imaging studies were also helpful in distinguishing subgroups; although not part of the variable criteria to differentiate MELAS subgroups, patients with atypical MELAS showed new lesions and more severe progression of the atrophy in short follow-up studies, supporting the more severe clinical outcome noted in this group.

Although there were several key differences distinguishing the 2 groups, all 35 individuals with MELAS in our cohort met the MELAS diagnostic criteria. In addition, 2 individuals, 1 from each group (classic and atypical), showed similar findings from histologic analysis, further supporting the groups having shared similar pathophysiology.<sup>29</sup> The underlying pathophysiology of acute SLE of MELAS has been elucidated during the past few decades, with a major role related to altered nitric oxide metabolism causing vascular endothelium dysfunction.<sup>24,30</sup> Overall, less nitric oxide is present in patients with MELAS due to excess cytochrome c oxidase in smooth-muscle binding to nitric oxide.<sup>24,30</sup> Therefore, MELAS places the individual at risk of SLE, especially during periods of increased metabolic demand due to physiologic stressors.

The lesions may respond to specific therapy management, particularly in the context of drugs implicated in the nitric oxide pathway, such as arginine. These drugs have been considered as a treatment for these patients, but there are currently no FDA-approved medications for MELAS treatment, primarily because there is a large outcome variability without a predictable response to the drugs. Using homogeneous subgroups in clinical trials, classic MELAS versus atypical MELAS, will likely be an important factor contributing to drug development and in predicting a response to therapeutic interventions. For promising future results, the patient population must be carefully phenotyped; the natural history of the disease, well understood; and the patient's health, optimized for trial readiness.<sup>31</sup>

The main limitation of this study is the potential bias from the challenge of clinically diagnosing mitochondrial disorders. To avoid the inclusion of patients without MELAS, a neurologist performed a clinical chart review to confirm that each patient fulfilled the established MELAS criteria, despite the presence of other symptoms or clinical overlap syndromes. Because the MELAS diagnosis is also based on radiologic appearance, our study meets a crucial need by expanding the radiologic-phenotype spectrum of this disorder beyond that of existing literature. Another limitation is that the sample size is relatively small. This small size was due to our preference for using rigorous inclusion criteria, recruiting only those patients with a definitive diagnosis of MELAS; a full set of clinical, genetic, laboratory, and MR imaging data available for review; and mtDNA pathogenic variants, because the pathophysiology of the mtDNA replication defect should be considered distinct from nuclear DNA disorders.

## CONCLUSIONS

Overall, we have identified a composite set of parameters that collectively serve as a clinical biomarker for distinguishing classic

and atypical subgroups of MELAS. These subgroups should be prospectively validated in future natural history studies and may be used in interventional clinical trials for defining clinical and neuroimaging phenotypes and correlating these with underlying gene etiologies and, ultimately, candidate treatment outcomes.

## ACKNOWLEDGMENTS

We thank the patients and their families for their involvement. We also thank Victoria A. Ramirez (PSM, Medical Science Writer at the Department of Radiology, Children's Hospital of Philadelphia) for providing editorial support for this article.

Disclosure forms provided by the authors are available with the full text and PDF of this article at [www.ajnr.org](http://www.ajnr.org).

## REFERENCES

1. Finsterer J. **Mitochondrial metabolic stroke: phenotype and genetics of stroke-like episodes.** *J Neurol Sci* 2019;400:135–41 [CrossRef Medline](#)
2. Lu JQ, Tarnopolsky MA. **Mitochondrial neuropathy and neurogenic features in mitochondrial myopathy.** *Mitochondrion* 2021;56:52–61 [CrossRef Medline](#)
3. Chakrabarty S, Govindaraj P, Sankaran BP, et al. **Contribution of nuclear and mitochondrial gene mutations in mitochondrial encephalopathy, lactic acidosis, and stroke-like episodes (MELAS) syndrome.** *J Neurol* 2021;268:2192–207 [CrossRef Medline](#)
4. Wei X, Du M, Li D, et al. **Mutations in FASTKD2 are associated with mitochondrial disease with multi-OXPHOS deficiency.** *Hum Mutat* 2020;41:961–72 [CrossRef Medline](#)
5. Yoo DH, Choi YC, Nam DE, et al. **Identification of FASTKD2 compound heterozygous mutations as the underlying cause of autosomal recessive MELAS-like syndrome.** *Mitochondrion* 2017;35:54–58 [CrossRef Medline](#)
6. Yatsuga S, Povalko N, Nishioka J, et al; Taro Matsuoka for MELAS Study Group in Japan. **MELAS: a nationwide prospective cohort study of 96 patients in Japan.** *Biochim Biophys Acta* 2012;1820:619–24 [CrossRef Medline](#)
7. Hirano M, Ricci E, Koenigsberger MR, et al. **Melas: an original case and clinical criteria for diagnosis.** *Neuromuscul Disord* 1992;2:125–35 [CrossRef Medline](#)
8. Sproule DM, Kaufmann P. **Mitochondrial encephalopathy, lactic acidosis, and stroke-like episodes: basic concepts, clinical phenotype, and therapeutic management of MELAS syndrome.** *Ann N Y Acad Sci* 2008;1142:133–58 [CrossRef Medline](#)
9. Alves CA, Teixeira SR, Martin-Saavedra JS, et al. **Pediatric Leigh syndrome: neuroimaging features and genetic correlations.** *Ann Neurol* 2020;88:218–32 [CrossRef Medline](#)
10. Goto Y, Nonaka I, Horai S. **A mutation in the tRNA(Leu)(UUR) gene associated with the MELAS subgroup of mitochondrial encephalomyopathies.** *Nature* 1990;348:651–53 [CrossRef Medline](#)
11. Karicheva OZ, Kolesnikova OA, Schirtz T, et al. **Correction of the consequences of mitochondrial 3243A>G mutation in the MT-TL1 gene causing the MELAS syndrome by tRNA import into mitochondria.** *Nucleic Acids Res* 2011;39:8173–86 [CrossRef Medline](#)
12. Chin J, Marotta R, Chiotis M, et al. **Detection rates and phenotypic spectrum of m. 3243A>G in the MT-TL1 gene: a molecular diagnostic laboratory perspective.** *Mitochondrion* 2014;17:34–41 [CrossRef Medline](#)
13. Pickett SJ, Grady JP, Ng YS, et al. **Phenotypic heterogeneity in m.3243A>G mitochondrial disease: the role of nuclear factors.** *Ann Clin Transl Neurol* 2018;5:333–45 [CrossRef Medline](#)
14. Nesbitt V, Pitceathly RD, Turnbull DM, et al. **The UK MRC Mitochondrial Disease Patient Cohort Study: clinical phenotypes associated with the m.3243A>G mutation—implications for diagnosis**

- and management. *J Neurol Neurosurg Psychiatry* 2013;84:936–38 [CrossRef Medline](#)
15. Miyahara H, Matsumoto S, Mokuno K, et al. **Autopsied case with MERRF/MELAS overlap syndrome accompanied by stroke-like episodes localized to the precentral gyrus.** *Neuropathology* 2019;39:212–17 [CrossRef Medline](#)
  16. Malfatti E, Bugiani M, Invernizzi F, et al. **Novel mutations of ND genes in complex I deficiency associated with mitochondrial encephalopathy.** *Brain* 2007;130:1894–904 [CrossRef Medline](#)
  17. Mezuki S, Fukuda K, Matsushita T, et al. **Isolated and repeated stroke-like episodes in a middle-aged man with a mitochondrial ND3 T10158C mutation: a case report.** *BMC Neurol* 2017;17:217 [CrossRef Medline](#)
  18. von Elm E, Altman DG, Egger M, et al; STROBE Initiative. **The Strengthening the Reporting of Observational Studies in Epidemiology (STROBE) statement: guidelines for reporting observational studies.** *Lancet* 2007;20:1453–7 [CrossRef Medline](#)
  19. Rahman S, Poulton J, Marchington D, et al. **Decrease of 3243 A→G mtDNA mutation from blood in MELAS syndrome: a longitudinal study.** *Am J Hum Genet* 2001;68:238–40 [CrossRef Medline](#)
  20. Ng YS, Lax NZ, Blain AP, et al. **Forecasting stroke-like episodes and outcomes in mitochondrial disease.** *Brain* 2022;145:542–54 [CrossRef Medline](#)
  21. Rahman S, Copeland WC. **POLG-related disorders and their neurological manifestations.** *Nat Rev Neurol* 2019;15:40–52 [CrossRef Medline](#)
  22. Ishigaki H, Sato N, Kimura Y, et al. **Linear cortical cystic lesions: characteristic MR findings in MELAS patients.** *Brain Dev* 2021;43:931–38 [CrossRef Medline](#)
  23. Di Stadio A, Pegoraro V, Giaretta L, et al. **Hearing impairment in MELAS: new prospective in clinical use of microRNA, a systematic review.** *Orphanet J Rare Dis* 2018;13:35 [CrossRef Medline](#)
  24. El-Hattab AW, Adesina AM, Jones J, et al. **MELAS syndrome: clinical manifestations, pathogenesis, and treatment options.** *Mol Genet Metab* 2015;116:4–12 [CrossRef Medline](#)
  25. Chae HW, Na JH, Kim HS, et al. **Mitochondrial diabetes and mitochondrial DNA mutation load in MELAS syndrome.** *Eur J Endocrinol* 2020;183:505–12 [CrossRef Medline](#)
  26. Cho JH, Kim JH, Choi JH, et al. **Endocrine dysfunctions in patients with mitochondrial diseases.** *Int J Pediatr Endocrinol* 2015;2015:O23 [CrossRef](#)
  27. Rahman J, Rahman S. **Mitochondrial medicine in the omics era.** *Lancet* 2018;391:2560–74 [CrossRef Medline](#)
  28. Bhatia KD, Krishnan P, Kortman H, et al. **Acute cortical lesions in MELAS syndrome: Anatomic distribution, symmetry, and evolution.** *AJNR Am J Neuroradiol* 2020;41:167–73 [CrossRef Medline](#)
  29. Betts J, Jaros E, Perry RH, et al. **Molecular neuropathology of MELAS: level of heteroplasmy in individual neurones and evidence of extensive vascular involvement.** *Neuropathol Appl Neurobiol* 2006;32:359–73 [CrossRef Medline](#)
  30. El-Hattab AW, Jahoor F. **Assessment of nitric oxide production in mitochondrial encephalomyopathy, lactic acidosis, and stroke-like episodes syndrome with the use of a stable isotope tracer infusion technique.** *J Nutr* 2017;147:1251–57 [CrossRef Medline](#)
  31. Goldstein A, Rahman S. **Seeking impact: global perspectives on outcome measure selection for translational and clinical research for primary mitochondrial disorders.** *J Inherit Metab Dis* 2021;44:343–57 [CrossRef Medline](#)